Sugar Specificity of Human β-Cell Glucokinase: Correlation of Molecular Models with Kinetic Measurements†

Liang Zhong Xu,‡ Irene T. Weber,§ Robert W. Harrison,§ Madhavi Gidh-Jain,‡ and Simon J. Pilkis*,‖

Department of Physiology and Biophysics, Health Science Center, SUNY at Stony Brook, Stony Brook, New York 11794, Department of Pharmacology, Jefferson Cancer Institute, Thomas Jefferson University, Philadelphia, Pennsylvania 19107, and Department of Biochemistry, University of Minnesota, Minneapolis, Minnesota 55455

Received October 20, 1994; Revised Manuscript Received February 17, 1995⊗

ABSTRACT: Human β-cell glucokinase recognition and phosphorylation of different sugars was investigated by steady-state kinetic analysis, measurements of substrate-induced intrinsic fluorescence changes, and molecular modeling and calculation of interaction energies. Measurements of k_{cat}/K_m showed that glucokinase phosphorylated the sugars in the order glucose = mannose > deoxyglucose > fructose = glucosamine. The mode of binding of these sugars to the open conformation of glucokinase was predicted from molecular modeling. Glucokinase is predicted to form similar interactions with the 6-OH, 4-OH, and 1-OH groups of all these sugars. The interactions of the 2-OH and 3-OH groups differ and depend on the type of sugar and reflect differences in cooperative behavior. For example, glucose and deoxyglucose exhibited cooperative behavior with Hill coefficients of 1.8 and 1.5, respectively, while mannose and fructose demonstrated Michaelis−Menten behavior. Galactose, allose, and 2,5-anhydroglucitol were not substrates under the assay conditions used, and the α- and β-anomers of methylglucose were poor substrates with K_m's greater than 1000 mM. Glucokinase exhibited an ATPase activity which was 1/2000th that of the rate of the kinase reaction, and unlike yeast hexokinase, it was not affected by the addition of lyxose. Glucosamine was a low affinity inhibitor as well as a substrate, while *N*-acetylglucosamine and mannoheptulose were high-affinity inhibitors. The change in intrinsic fluorescence that was induced by glucose, mannose, and mannoheptulose had the opposite sign for glucosamine, which implies a very different mode of binding from the other sugars. The calculated interaction energies of glucokinase with glucose, mannose, deoxyglucose, and fructose agree very well with the measured values of k_{cat}/K_m, which indicates that these sugars are recognized by binding to the open conformation of glucokinase.

Glucokinase (ATP:D-hexose-6-phosphotransferase, EC 2.7.1.2.) or hexokinase type IV catalyzes the phosphorylation of glucose, the first rate-limiting reaction in glycolysis (Weinhouse, 1976; Meglasson, 1986; Granner & Pilkis, 1990). It is expressed in the pancreatic β-cells and liver and is readily distinguished from other hexokinases in mammalian cells by its smaller size (50 kDa), an affinity for glucose (K_m = 6 mM) that is lower than other hexokinase isozymes (20−130 μM) and within the physiological range of plasma glucose levels, and a relative lack of inhibition by glucose 6-phosphate. These properties ensure a gradient for glucose entry into the hepatocyte and β-cells, especially following a meal when plasma glucose levels are elevated.

Recent studies have shown that mutations in glucokinase can lead to the development of an autosomal dominant form of non-insulin-dependent diabetes that has an onset in childhood (Vionnet et al., 1992; Stoffel et al., 1992a,b; Polonsky et al., 1986). Clinical studies have demonstrated that the threshold for glucose-stimulated insulin secretion in subjects with glucokinase mutations is increased, implying that the mutations affect glucose sensing by the pancreatic β-cells (Sturis et al., 1994). We have previously reported the effects of a number of missense mutations on the enzymatic properties of human β-cell glucokinase, and all are associated with a decrease in V_{max} and/or in affinity for glucose (Gidh-Jain et al., 1993; Takeda et al., 1993). Many of these mutations were in regions of the protein encoded by exons 5, 7, and 8 (Gidh-Jain et al., 1993; Takeda et al., 1993), and molecular modeling (Harrison, 1985; Charles et al., 1994) predicted that they are in the active site cleft or in surface loops leading into this cleft as well as in a region of the smaller of the two glucose domains of the glucokinase molecule that is believed to undergo a substrate-induced conformation change. A model of human β-cell glucokinase has been constructed based on the crystal structure of yeast hexokinase B that predicts which residues form the glucose binding site (Harrison, 1985; Charles et al., 1994). However, while the sugar specificity of the rat liver glucokinase has been investigated and kinetic models for sigmoid behavior of the enzyme have been presented (Neet et al., 1990; Cardenas et al., 1984a,b), a functional analysis of sugar specificity of the human β-cell glucokinase has not been undertaken. In order to understand the molecular basis for the sugar specificity of human glucokinase, molecular models of different sugars bound to the enzyme have been built. These studies complement our parallel experiments using site-directed mutagenesis of residues in the sugar binding site of glucokinase (Xu et al., 1994b). The improved models for human glucokinase described here resulted from more

† This work was supported by National Institutes of Health Grant DK 38354.

* Telephone: 612/625-6100; FAX: 612/625-2163; e-mail address: pilkis@brain.biochem.umn.edu.

‡ SUNY at Stony Brook.

§ Thomas Jefferson University.

‖ University of Minnesota.

⊗ Abstract published in *Advance ACS Abstracts,* April 15, 1995.

0006-2960/95/0434-6083$09.00/0

accurate energy minimization using all-atom potentials, no cutoff limits, and solvent from the yeast hexokinase crystal structure. This new minimization of the model allowed calculation of the glucokinase−sugar interaction energies, which could then be compared with kinetic measurements and fluorescence analyses for the four substrates: glucose, mannose, 2-deoxyglucose, and fructose.

EXPERIMENTAL PROCEDURES

Materials. Q-Sepharose was from Pharmacia LKB Biotechnology Inc. Glucose-6-phosphate dehydrogenase, lactate dehydrogenase, and pyruvate kinase were from Boehringer Mannheim. Glucosamine, *N*-acetylglucosamine, mannose, fructose, allose, galactose, and all other sugars were from Sigma.

Construction of pET Expression Plasmids for Human β-Cell Glucokinase. A 2.6-kb human pancreatic β-cell glucokinase cDNA clone (Gidh-Jain et al., 1993), ph-GK-20, was used to generate the construct pEhgk-WT. An *Nde*I site was generated at the 5′ end using the polymerase chain reaction with an oligonucleotide that has a one base pair mismatch (GGC TGG TGT GCA TAT GCT GGA CGA CAG). The insert in the pET 3a expression construct included the protein coding region of the cDNA as well as the 3′-untranslated region.

Bacterial Expression and Purification of Native of Human β-Cell and Liver Glucokinase. Glucokinase was expressed in *Escherichia coli* BL21 (DE3)-plys S using the phage T7 RNA polymerase-based system (Studier & Moffat, 1986) except that a lower induction temperature was used (Lin et al., 1990; Lange et al., 1991). The yield of β-cell glucokinase was about 20 mg/L while the yield of the liver enzyme was 80 mg/L. Cell extracts containing glucokinase were subjected to freeze-thawing three times to break the cells, and 100 μg/mL DNase A and 1 mg/mL lyzozyme were added to the cell extract at 4 °C for 1 h. Glucokinase was purified by a modification of previously published procedures (Takeda et al., 1993). Briefly, the enzyme was first partially purified by precipitation with 40−65% $(NH_4)_2SO_4$. The pellet was dissolved in glucokinase buffer (50 mM KP_i, pH 8.0, 1 mM EDTA, 1 mM DTT, and 0.5 mM PMSF), dialyzed against the same buffer, and then loaded on to a 100-mL Q-Sepharose column. The column was washed with 2 L of glucokinase buffer containing 150 mM KCl, and the enzyme was eluted with a linear gradient of 150−450 mM KCl. The fractions containing enzyme activity were pooled, precipitated with 70% $(NH_4)_2SO_4$, and dissolved in 1 mL of glucokinase buffer. Glucokinase was loaded on to a −100 mL G-100 Sephadex superfine column equilibrated in glucokinase buffer and eluted from the column with an apparent molecular weight of 50 kDa. Native human β-cell glucokinase has a specific activity of about 80−120 units/mg, which is similar to that reported for the purified rat liver enzyme (Andreone et al., 1989).

Enzyme Assay and Kinetic Analysis. Glucokinase activity was assayed at 30 °C by measuring the increase in absorbance of NADPH at 340 nm in a coupled enzyme system, which employed Glu-6-P dehydrogenase as described previously (Lange et al., 1991). The Glu-6-P dehydrogenase assay was used to determine the K_i's for *N*-acetylglucosamine and mannoheptulose. When sugar specificity was studied, glucokinase activity was measured by monitoring the decrease in absorbance at 340 nm in a assay mixture containing 100 mM Tris-HCl (pH 7.5), 100 mM KCl, 20 mM $MgCl_2$, 0.6 mM P-enolpyruvate, 0.2 mM NADH, 1 mM ATP, 1.76 unit/mL lactate dehydrogenase, and 1.4 units/mL pyruvate kinase. When glucosamine was used as a substrate, the assay mixture and glucosamine were adjusted to pH 9.0, and the lactate dehydrogenase and pyruvate kinase coupling assay was used to determine K_m and K_i for glucosamine. Calculations of V_{max} and K_m for substrates were obtained by the nonlinear least square fitting program to fit a Michaelis−Menten equation or $V = V_{max}S^n/(K_m + S^n)$ for the Hill coefficient n using a σ plot.

Molecular Modeling and Energy Calculations. The initial model for the structure of glucokinase was built as reported previously (Charles et al., 1994). Additional modeling, energy minimization, and calculation of sugar−glucokinase interaction energies were all performed with the program AMMP (Harrison, 1993). In order to increase the accuracy of the calculations, hydrogen atoms were included by using an all-atom potential, and no cutoff was used for the electrostatic and nonbonded terms. The water molecules from the refined crystal structure of yeast hexokinase B (Harrison, 1985) were included in the new model for glucokinase with sugar. Inclusion of these water molecules was found to be important since in their absence the minimized model deviated more from the crystal structure in the region of the glucose-binding site. The structure of α-D-glucose was based on the structure of the inhibitor, *o*-tolulylglucosamine (OTG),[1] from the high-resolution crystal strcture of yeast hexokinase B. The model structures of the other sugars (mannose, 2-deoxyglucose, fructose, mannoheptulose, glucosamine, and *N*-acetylglucosamine) were built using AMMP, and the conformation was checked by examination in the Evans and Sutherland ESV10 AMMP computer graphics system running the program FRODO (Jones, 1985). The positions of all new atoms were calculated in AMMP during energy minimization. Energy minimization was done with alterations of short runs of molecular dynamics and conjugate gradients. The UFF all-atom potentials (Rappe et al., 1992) were used with charges taken from the AMBER all-atom set (Weiner et al., 1986). Charges for the sugars were generated with the method of moments version of QEq (Rappe & Goddard, 1991) as implemented in AMMP. A version of the fast multipole method was used to calculate the electrostatic and nonbonded terms. No cutoff was applied for nonbonded and electrostatic terms. The amortized calculation of nonbonded terms that is implemented in AMMP performed this calculation efficiently by sharing the cost over many energy and force calculations. The potential due to the distal (more than 6 Å) atoms was expanded in a quadratic power series. The local atom terms were always recalculated. When any atom had moved more than 1.0 Å during dynamics, the distal terms were recalculated. During minimization, the update of distal terms occurred every 30 steps of conjugate gradients. The mixed treatment of nonbonded and electrostatic terms gives good asymptotic treatment of the total potential and runs with no cutoff in times close to those of the more standard treatment using a 8−10-Å cutoff radius. The exact time savings depends on how often the distal terms are updated. The combined approach is especially powerful during

[1] Abbreviations: *o*-tolulylglucosamine, (OTG); dithiothreitol, DTT.

conjugate gradient optimization and runs in times close to those with a 6-Å cutoff. Alternating conjugate gradients minimization and short (20−40 fs) molecular dynamics runs were used for the final optimization. Conjugate gradients minimization of nonquadratic functions exhibits stagnation at saddle points and local singularities of the potential. The short runs of molecular dynamics serve to move the coordinates away from these points and thus aid convergence. In addition, for glucosamine and *N*-acetylglucosamine, a torsion search was applied to the 2-amide and the acetyl group as appropriate. Finally, the minimized model was analyzed to calculate the nonbonded and electrostatic terms for the interaction between glucokinase and each type of sugar. The structures with the different sugars were compared, and the sugar−glucokinase interactions are listed.

Determination of Intrinsic Fluorescence of β-Cell Glucokinase. Experiments were performed in a buffer containing 50 mM KP_i, pH 7.5, 1 mM $MgCl_2$, 1 mM EDTA, 1 mM DTT, and 5% glycerol with a multifrequency phase fluorometer (ISS Inc.). The excitation wavelengths were 280 nm in a 10 × 10 mm^2 size cuvet (Lin & Neet, 1990). Glucose was removed from glucokinase prior to the experiment by a dialysis overnight against a buffer containing 50 mM KP_i, pH 7.5, 1 mM EDTA, and 1 mM DDT. The experiment was initiated by the addition of a final concentration of 100 mM hexose. The fluorescence spectra were recorded after the addition of sugar and then analyzed with an IBM-PC microcomputer interfaced with the fluorometer to extract maximum fluorescence intensity of spectra at 312 nm. The relative fluorescence enhancement was obtained by dividing fluorescence enhancement by the initial intrinsic fluorescence. Relative fluorescence enhancement measurements were normalized by carrying out control experiments in which buffer instead of hexose was added.

Assay of ATPase Activity of Glucokinase. Reaction mixtures for following the ATPase activity of glucokinase contained 0−20 mM Mg [γ-^{32}P]ATP (3 × 10^5 cpm/μmol), 5 mM excess $MgCl_2$, 50 mM Pipes, pH 7.0, and 20 μg of glucokinase in 200 μL. Aliquots of 100 μL were removed at 0.5 and 1 h and added to 100 μL of a solution containing 1.25% NaCl and 1.25% ammonium molybdate in 0.25 N H_2SO_4. 2-Butanol (200 μL) was added, and the solution was vortexed. A 100-μL aliquot of the 2-butanol layer was removed and counted to determine the inorganic phosphate formed (Viola et al., 1982).

RESULTS

Expression and Purification of the Human β-Cell and Liver Glucokinases. Human β-cell and liver glucokinase were expressed in *E. coli* using the pET expression system and purified 20-fold from extracts of *E. coli* by $(NH_4)_2SO_4$ precipitation (45−65%), Q-Sepharose chromatography, and gel filtration on Sephadex G-100 superfine as described under Experimental Procedures. A summary of the purification scheme for the β-cell glucokinase is shown in Table 1. The Q-Sepharose column is the most important step since it removes contaminating bacterial hexokinase activity. The enzyme was homogeneous as judged by SDS−PAGE (Figure 1). Native human β-cell and liver glucokinase had specific activities of about 80 unit/mg. Comparison of kinetic properties of human liver (K_m for glucose = 6.0 mM, K_m for ATP = 0.51 mM, V_{max} = 80 unit/mg, and Hill coefficient = 1.85) and β-cell glucokinases revealed no significant differences with respect to K_m for glucose or ATP, V_{max}, and Hill coefficient. The kinetic properties were identical even though the isozymes differ greatly in the first 20 NH_2-terminal amino acids.

Table 1: Summary of the Purification Scheme for Human β-Cell Glucokinase[a]

step	total acty (units/L)	sp acty (units/mg)	purification fold (fold)	yield (%)
crude extract	800	0.9	1	100
$(NH_4)_2SO_4$ 45−65%	800	5	5.5	90
Q-Sepharose	320	50	50	40
Sephadex G-100	160	80	90	50

[a] One liter of cells containing the glucokinase expression plasmid was induced at 22 °C with IPTG and extracted by freeze-thawing three times. The cell extract was fractionated with 40−65% $(NH_4)_2SO_4$. The ammonium sulfate pellet was dissolved in glucokinase buffer (50 mM KP_i, pH 8.0, 1 mM EDTA, and 10 mM glucose) and dialyzed against the same buffer overnight and loaded onto a 100-mL Q-Sepharose column. The Q-Sepharose column was washed extensively and eluted with a linear gradient of 150−450 mM KCl. The fractions containing glucokinase activity were pooled and then purified to homogenity on a Sephadex G-100 superfine column.

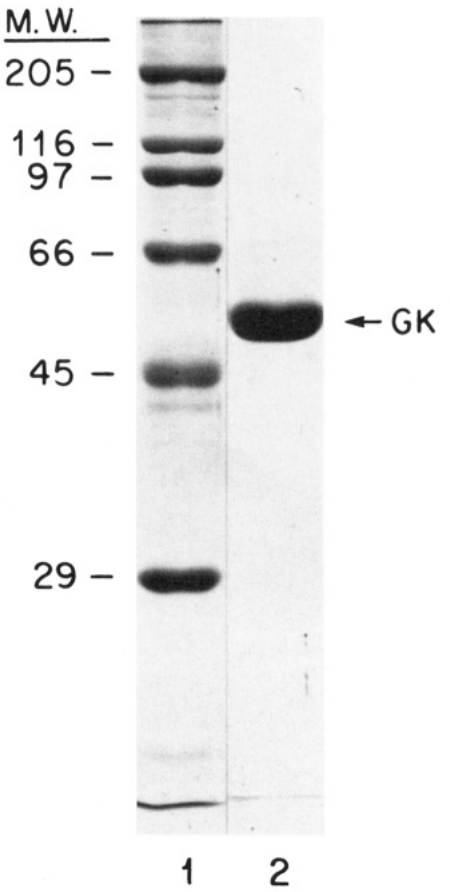

FIGURE 1: SDS−PAGE of human β-cell glucokinase. About 10 μg of glucokinase was subjected to SDS−PAGE. The first lane contained standard molecular size markers, and lane 2 contained human β-cell glucokinase. The gel was stained with Coomassie Blue.

Sugar Specificity of Human β-Cell Glucokinase. Glucose, mannose, and 2-deoxyglucose are all good substrates of β-cell glucokinase (Table 2). They differ only in the 2-OH position, which suggests that the presence of the 2-OH and its conformation are not important for efficient phosphorylation. K_m values have been used to compare the relative

Table 2: Kinetic Study of Human β-Cell Glucokinase with Various Sugars[a]

sugars	K_m (mM)	rel *V/V* glucose (%)	Hill coeff	K_i (mM)
glucose	6.03 ± 0.34[b]	100	1.78 ± 0.04	
2-deoxyglucose	18 ± 2.50[b]	85	1.47 ± 0.16	
mannose	4.35 ± 0.34	84	1.12 ± 0.14	
fructose	240 ± 29	176	1.06 ± 0.12	
galactose		no activity[c]		
allose		no activity[d]		
methyl-α-glucopyranose	>1000	4.9[c]		
methyl-β-glucopyranose	>1000	1.3[c]		
2,5-anhydroglucitol		no activity[c]		
glucosamine[e]	61 ± 20	30		47 ± 16
N-acetylglucosamine	no activity			0.20
mannoheptulose		no activity		0.76

[a] Glucokinase activity was measured by monitoring the increase in NADPH using glucose-6-phosphate dehydrogenase coupling assay or by monitoring the decrease in NADPH using the lactate dehydrogenase/pyruvate kinase coupled assay as described in Experimental Procedures. The relative *V/V* values for sugars were obtained from V_{max} using saturating concentrations of the sugars and the V_{max} using saturating concentrations of glucose. V_{max}, K_m, and the Hill coefficient were determined by nonlinear least square routines using an equation of $V = V_{max}S^n/(K_m + S^n)$. K_i was obtained from a competitive inhibition equation of $K_m' = K_m(1 + [I]/K_i)$. [b] Values reported are actually $S_{0.5}$ because of kinetic sigmoid behavior. [c] Values reported were measured at 500 mM concentration. [d] Value reported was measured at 100 mM concentration. [e] Values were obtained by curve fitting to the equation $v = V_{max}S/(K_m + S + S^2/K_i)$ (Cleland, 1979). The kinetic constants for glucosamine were obtained at pH 9.0. The auxiliary enzymes in the pyruvate kinase/LDH assay mixture were not rate limiting at any pH tested.

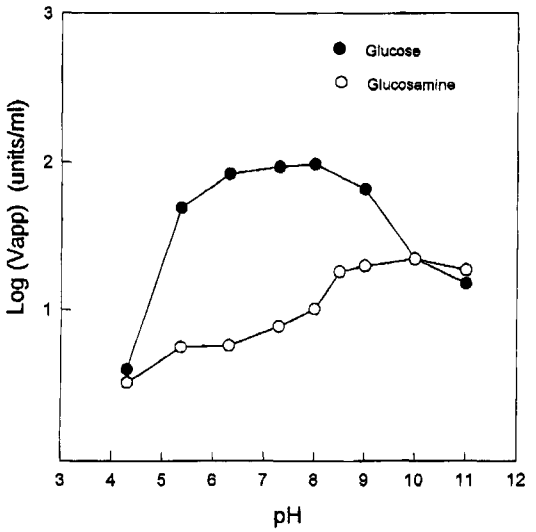

FIGURE 2: pH kinetics of glucokinase using glucose and glucosamine as substrates. Glucokinase activity was measured by following ADP production using the pyruvate–lactate dehydrogenase coupling assays containing 100 mM glucose (1) or 100 mM glucosamine and 1 mM ATP. Two different buffer systems were used to cover the pH range 4–11: 100 mM TES was used for pH 4.0–7.5, and 100 mM Tris was used for pH 8.0–11.0.

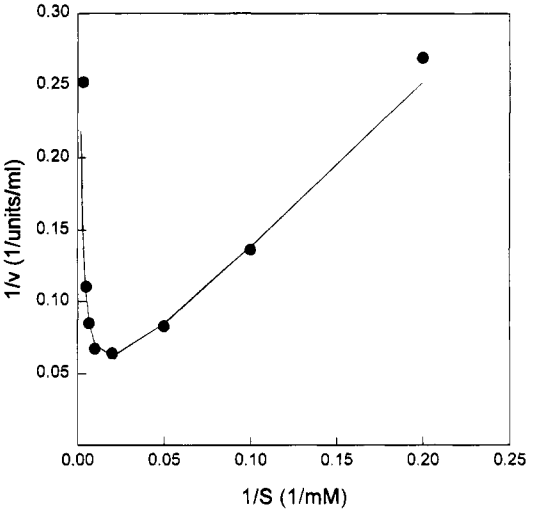

FIGURE 3: Glucosamine concentration dependence for human β-cell glucokinase activity and inhibition. The glucokinase activity was measured by following ADP production with the pyruvate kinase–lactate dehydrogenase coupled assay. About 12 different glucosamine concentrations in the range of 0–500 mM were used. The assays were performed at pH 9.0.

affinities of substrates; however, the K_m does not necessarily reflect the binding affinity. Fructose (K_m = 250 mM and k_{cat} = 116.9 s^{-1}) is also a substrate of glucokinase, which demonstrates that phosphorylation of both glucopyranose and fructopyranose can occur. As judged by the K_m determinations (Table 2), the enzyme's affinity for hexoses is in the following decreasing order: mannose ≥ glucose > deoxyglucose > fructose. Calculation of k_{cat}/K_m showed that specificity for glucokinase phosphorylation of the sugars was in the order glucose = mannose > deoxyglucose > fructose = glucosamine. Neither allose or galactose were substrates, which suggests that the orientation of the 3- and 4-hydroxyl groups are critical for phospho transfer because allose and galactose differ from glucose only in the orientation of the 3-OH or the 4-OH. Glucokinase activities with 500 mM methyl-α-glucopyranose or methyl-β-glucopyranose were 4.9% and 1.3% of that with 100 mM glucose, respectively. These results suggest that the 1-OH group is critical for sugar binding and phosphorylation because methylation of the 1-OH group greatly increased the K_m value to greater than 1000 mM. In addition, 2,5-anhydroglucitol was not a substrate (Table 2).

Glucosamine Dependence of β-Cell Glucokinase. Glucosamine is a substrate of the β-cell enzyme and shows substrate inhibition at high concentration (Table 2). Since glucosamine has a 2-NH_2 group, which has a pK_a around 8.0, it was of interest to analyze the pH dependence of sugar phosphorylation. The pH profile showed that with glucose as substrate the enzyme was active between pH 6 and pH 9, with an optimum between 7.5 and 8.0 (Figure 2). With glucosamine as substrate, glucokinase was only active above pH 8.0, with an optimum around pH 8.5–9.0, which suggests that the free amino form of glucosamine is the preferred substrate (see Figure 2). Therefore, pH 9.0 was chosen to analyze the kinetic parameters of glucosamine phosphorylation. From the velocity versus glucosamine concentration plot, glucosamine is a substrate of glucokinase, reaching

Table 3: Glucokinase Intrinsic Fluorescence Enhancement[a]

sugars	fluorescence enhancement (%)	sugars	fluorescence enhancement (%)
control	100.0 ± 2.6	glucosamine	35.0 ± 3.0
glucose	131.6 ± 3.9	fructose	80.4 ± 1.1
N-acetylglucosamine	121.3 ± 3.9	galactose	90.2 ± 2.0
mannose	132.9 ± 3.0	mannoheptulose	120.0 ± 1.5
2-deoxyglucose	120.5 ± 1.2		

[a] Glucokinase (WT) (10 μg) was added to buffer containing 50 mM KP_i, pH 7.5, 1 mM $MgCl_2$, 1 mM EDTA, 1 mM DTT, and 5% glycerol. The fluorescence spectra were recorded after the addition of a final concentration of 100 mM glucose or analogs with an IBM-PC microcomputer interfaced with the fluorometer and then analyzed to determine the maximum fluorescence intensity at approximately 312 nm. The relative fluorescence enhancement was obtained by dividing fluorescence enhancement by the initial intrinsic fluorescence. Relative fluorescence enhancement measurements were normalized by carrying out control experiments in which buffer instead of glucose was added.

highest activity at less than 100 mM (Figure 3). However, at glucosamine concentrations above 100 mM, substrate inhibition was observed with a K_i of 47 mM.

Competitive Inhibition by N-Acetylglucosamine and Mannoheptulose. *N*-Acetylglucosamine was a competitive inhibitor of human β-cell glucokinase (data not shown), confirming similar observations with other mammalian glucokinases (Neet et al., 1990). The K_i for *N*-acetylglucosamine was 0.2 mM (Table 2). Mannoheptulose has been used in vivo and in in vitro islet cell systems as an inhibitor of insulin secretion (Chan, 1993; Ferrer et al., 1993). Mannoheptulose was not a substrate of human β-cell glucokinase (data not shown) but rather was a competitive inhibitor with respect to glucose (data not shown) with a K_i of 0.7 mM (Table 2).

Sugar-Induced Changes in Intrinsic Fluorescence. Rat liver glucokinase exhibits a glucose-induced change in intrinsic fluorescence that has been postulated to reflect the presence of two different conformations of the enzyme (Lin & Neet, 1990). In the crystal structures, the yeast hexokinase enzyme is observed in an open conformation in the presence of a glucose analog inhibitor and in a closed conformation in the complex with glucose (Anderson et al., 1979). Human β-cell glucokinase is predicted to undergo a similar conformational change on the binding of glucose (Charles et al., 1994). The sugar-induced change can be demonstrated by measurements of the intrinsic fluorescence, as shown in Table 3 and Figure 4. In the absence of sugar substrate, glucokinase exhibited an intrinsic fluorescence with a peak at about 312 nm. At a substrate concentration of 100 mM, glucose, mannose, and 2-deoxyglucose induced an increase in intrinsic fluorescence, which suggests that the binding of each of these sugars induces a similar conformational change in glucokinase. Mannose and glucose increased the intrinsic fluorescence to very similar levels and also were phosphorylated with very similar values of k_{cat}/K_m (11.1 and 12.8). 2-Deoxyglucose induced a smaller change in fluorescence and was phosphorylated with a lower k_{cat}/K_m of 3.13. Fructose at 100 mM induced a decrease in fluorescence[2] and was phosphorylated with an even lower k_{cat}/K_m of 0.49. This is the first demonstration that fructose induces a change in fluorescence that has a different sign than for glucose, 2-deoxyglucose, and mannose. Glucosamine induced a large decrease in intrinsic fluorescence, which indicates that glucosamine

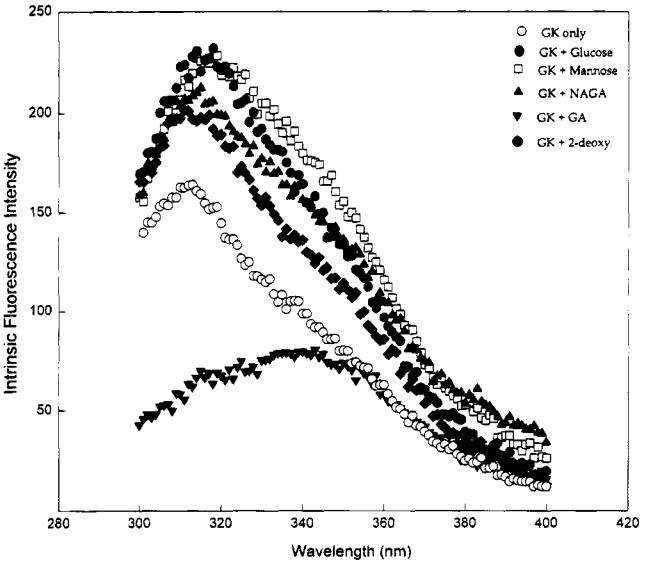

FIGURE 4: Effects of various sugars on the intrinsic fluorescence of glucokinase. Spectra were recorded as described in Experimental Procedures. Glucokinase wild type with buffer (●), 100 mM glucose (○), 100 mM glucosamine (▲), 100 mM *N*-acetylglucosamine (▼), 100 mM mannose (□), and 100 mM 2-deoxyglucose (♦).

produces a different type of conformational change to that predicted for glucose binding to glucokinase. Interestingly, the inhibitors, *N*-acetylglucosamine and mannoheptulose, also increased intrinsic fluorescence, which suggests that the conformational changes they induced were similar to that produced by glucose binding.

ATPase Activity of Human β-Cell Glucokinase. It has been shown that yeast hexokinase has low ATPase activity, which is 1/10,000th of the kinase activity. Yeast hexokinase ATPase activity is increased by sugar analogs such as lyxose or xylose (DelaFuente et al., 1970). It was of interest to determine whether β-cell glucokinase also has ATPase activity. As shown in Figure 5, human glucokinase had a low ATPase activity with a K_m for ATP of 4.5 mM and a V_{max} equal to 0.045 unit/mg. The K_m for ATP in ATPase reaction of glucokinase was 7-fold higher than the K_m for ATP in the kinase reaction (K_m = 0.63 mM). Concentrations of ATP above 10 mM inhibited the ATPase activity of glucokinase (Figure 5). Similar inhibition of the ATPase activity of yeast hexokinase by saturating concentrations of ATP were also observed (data not shown). The ATPase activity of glucokinase (0.04 unit/mg) was 1/2000th that of its kinase reaction. Lyxose (100 mM) had no effect on the ATPase activity of human β-cell glucokinase. Incubation of the enzyme with [γ-^{32}P]ATP at ATP concentration above 15 mM resulted in incorporation of ^{32}P into the enzyme to the extent of 0.1−0.2 mol of ^{32}P/mol of enzyme (data not shown).

Modeled Interactions of Glucokinase with the Different Sugars. The model of human glucokinase has been used to predict how the different sugars bind in the active site. The

[2] Higher concentrations of fructose (1800 mM) further decreased intrinsic fluorescence to values nearly equal to glucosamine. The molecular basis for the decreased intrinsic fluorescence with fructose is not clear, but may reflect the absence of any interaction with Glu-256, which is adjacent to Trp-257. All the other tested sugars and inhibitors have at least one potential hydrogen bond interaction with Glu-256.

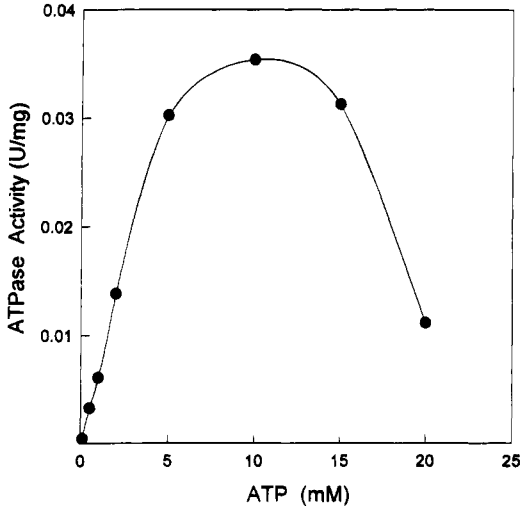

FIGURE 5: ATPase activity of human β-cell glucokinase. Glucokinase ATPase activity was measured by following the production of ^{32}P from [γ-^{32}P]ATP as described in Experimental Procedures. Eight different ATP concentrations in the range of 0−20 mM were used.

Table 4: Glucokinase Interaction with Different Sugars[a]

	k_{cat} (s^{-1})	K_m (mM)	k_{cat}/K_m	$-\ln(k_{cat}/K_m)$	energy (kcal/mol)
sugar					
glucose	66.4	6.03	11.07	−2.40	−76.05
mannose	56.4	4.35	12.82	−2.55	−75.46
2-deoxyglucose	56.4	18.0	3.13	−1.14	−62.73
fructose	116.9	240.0	0.49	0.72	−45.57
glucosamine	19.9	61.0	0.33	1.11	−65.99
N-acetylglucosamine					−67.8
mannoheptulose					−81.9

[a] The values for K_m are taken from Table 2, and the k_{cat} values were calculated from the relative V_{max} values in Tables 2 and at 66.4 s^{-1} for glucose. The interaction energies (in kcal/mol) for each of the glucokinase−sugar complexes were calculated from molecular models as described in Experimental Procedures.

four hexose sugars (glucose, 2-deoxyglucose, mannose, and fructose) are all phosphorylated by glucokinase. The pyranoses (glucose, mannose, and 2-deoxyglucose) have six-membered ring structures and differ in the position of the 2-hydroxyl group, while the furanose (fructose) has a five-membered ring structure. The model for human glucokinase in the open conformation was subjected to energy minimization in the presence of each type of sugar, and the glucokinase−sugar molecular mechanics interaction energy was calculated, as listed in Table 4. It was found to be important to include the water molecules observed in the crystal structure of yeast hexokinase in this model of human glucokinase. The minimized model structures were examined for the hydrogen bond interactions between glucokinase and the sugar hydroxyl groups, and the predicted binding sites for several different sugars are illustrated in Figure 6.

The glucose interactions with glucokinase are similar to those described previously for the model of glucokinase (Charles et al., 1994) and for the crystal structure of yeast hexokinase. Human glucokinase and yeast hexokinase are related by 31% identity in the amino acid sequences; however, the sugar-binding sites are highly conserved. This new model of glucose binding is more accurate than that reported previously (Charles et al., 1994) due to the inclusion of water molecules and the use of more accurate potentials

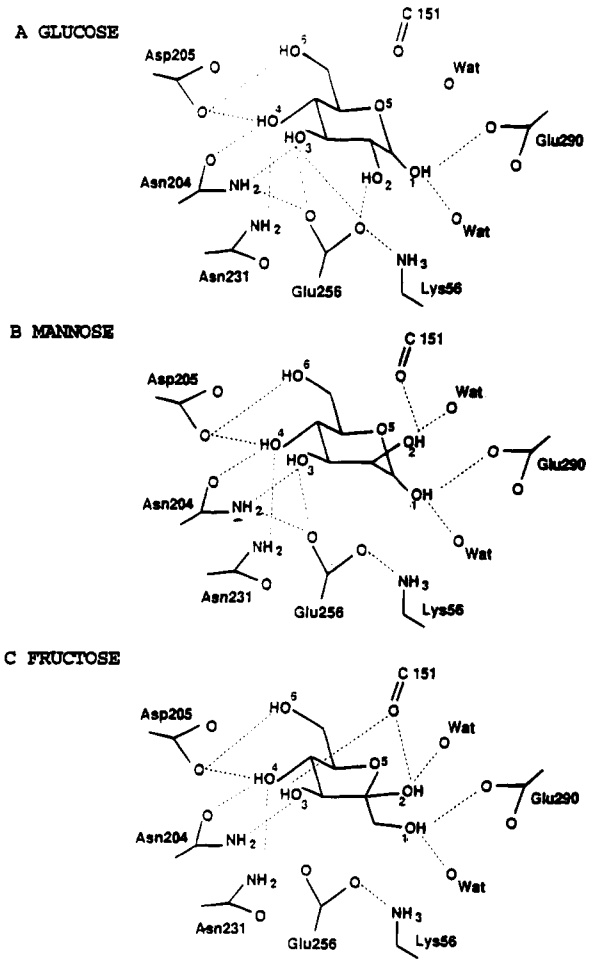

FIGURE 6: Hexose-binding site of human β-cell glucokinase. The amino acid residues and water molecules that are predicted to form hydrogen bond interactions with glucose, mannose, and fructose in the model glucokinase structure are shown. Potential hydrogen bonds are indicated by dashed lines.

with all hydrogen atoms and no cutoff limit for nonbonded and electrostatic interactions. All the hydroxyl groups of glucose form at least one hydrogen bond interaction with glucokinase residues (Figure 6a). The 1-OH interacts with the side chain oxygen of Glu-290 and with a water molecule that was observed in the crystal structure of yeast hexokinase B. The 2-OH interacts with the side chain oxygen of Glu-256, and the 3-OH interacts with Glu-256 and the amino group of Asn-204. The 4-OH shows three hydrogen bond interactions with the side chain atoms of Asn-204, Asp-205, and Asn-231, while the 6-OH formed a hydrogen bond interaction with Asp-205. In addition to these glucose−glucokinase hydrogen bonds, there are many hydrogen bonds that interconnect the glucokinase residues forming the sugar binding site. The interactions between the side chains of Asn-204 and Glu-256 and the salt bridge between Glu-256 and Lys-56 are shown in Figure 6a. Other interconnecting hydrogen bonds are not illustrated here for clarity. One difference in this model compared to the interactions that were observed for the crystal structure of yeast hexokinase is that the side chain of the catalytic Asp-205 has rotated to form a hydrogen bond with the 6-OH group, which is partially exposed to solvent. Small differences in the conformation of the catalytic residues on comparing the energy-minimized structure with the crystal structure have been noted previously, e.g., for HIV protease (Weber and

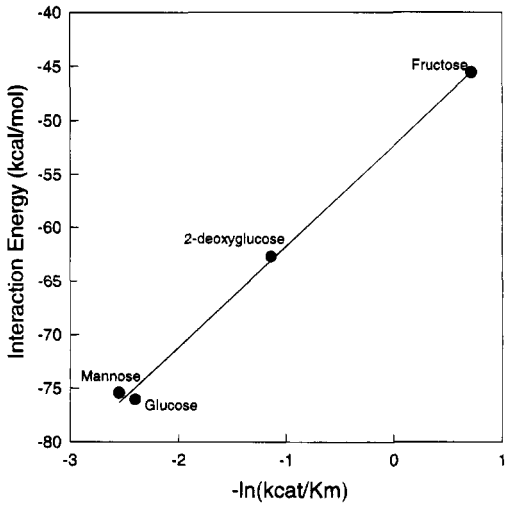

FIGURE 7: Plot of $-\ln (k_{cat}/K_m)$ versus calculated interaction energy (in kcal/mol) of different sugars and human β-cell glucokinase. The correlation coefficient is 0.99.

Harrison, unpublished results).

Deoxyglucose lacks the 2-OH group of glucose and is predicted to bind similarly to glucose, except that there is no equivalent of the glucose 2-OH interaction with Glu-256, which means that the calculated interaction energy is higher than for glucose. Glucosamine was modeled as binding in a manner very similar to that of glucose. These two sugars differ only in the group present at the 2-position. The 2-amino group of glucosamine formed a hydrogen bond interaction with the side chain oxygen of Glu-256, similar to that formed by the 2-OH of glucose (Figure 6a).

Mannose is predicted to bind in a similar manner to that of glucose, with the exception of the interaction formed by the 2-OH group (Figure 6b). Glucose and mannose differ only in the conformation of the 2-hydroxyl. The 2-OH of glucose interacts with the side chain of Glu-256 in the glucokinase binding site, while the 2-OH of mannose is predicted to form a hydrogen bond interaction with the carbonyl oxygen of residue 151 and with a water molecule instead.

Fructose has a five-membered ring structure rather than the six-membered ring of glucose. The model structure suggested that the interactions of the 6-OH, 1-OH, and 4-OH are similar in glucose and fructose (Figure 6c). The 3-OH group of fructose has moved compared to the 3-OH of glucose and does not form hydrogen bond interactions with Glu-256. The main differences are in the interactions of the 2-OH of glucose compared to fructose. In fact, the 2-OH group of fructose is predicted to interact with the carbonyl oxygen of residue 151 and with a water molecule, similar to the prediction for the 2-OH of mannose.

The calculated values of the interaction energy between the different sugars and glucokinase are shown in Table 4. The kinetic measurements for the four sugar substrates (glucose, 2-deoxyglucose, mannose and fructose) are compared to the calculated interaction energies in Figure 7. The interaction energies are plotted against values of $-\ln (k_{cat}/K_m)$, which will be proportional to the differences in free energy as estimated from the kinetic measurements ($\Delta G = -RT \ln k_{cat}/K_m$). The correlation coefficient between these parameters was 0.99. This excellent correlation suggested that the neglected energies of solvation and entropic effects are similar for these four sugar substrates.

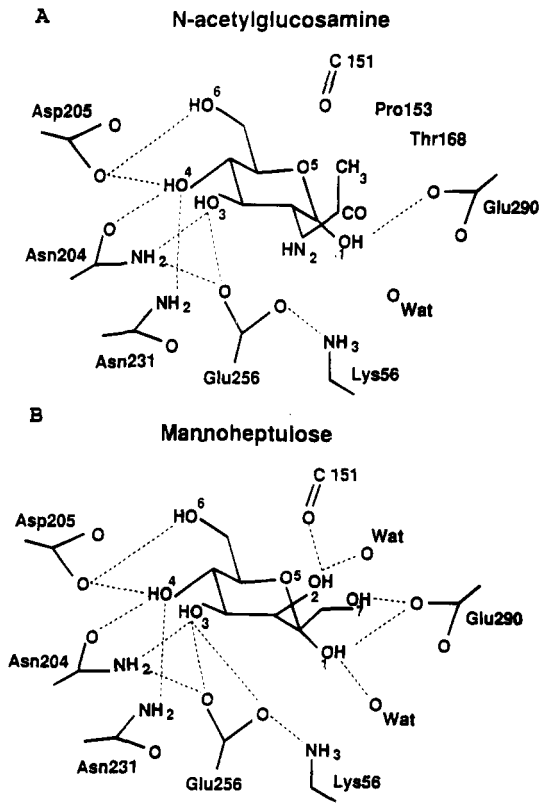

FIGURE 8: Postulated inhibitor binding to the hexose-binding site of human β-cell glucokinase: (A) *N*-acetylglucosamine; (B) mannoheptulose. The glucokinase residues and water molecules that are predicted to interact with these inhibitors are shown. Dashed lines indicate the potential hydrogen bond interactions.

Inhibitor Binding to Glucokinase. Two sugar-based inhibitors of glucokinase, *N*-acetylglucosamine and mannoheptulose, were modeled in the open conformation of glucokinase bound in the glucose-binding site. Analysis of the model complexes of glucokinase after energy minimization showed that the inhibitors had similar interactions with glucokinase as were described earlier for the sugar substrates. Similar hydrogen bond interactions were predicted for the 1-OH, 3-OH, 4-OH, and 6-OH groups of *N*-acetylglucosamine and glucose (Figure 8a). However, although the 2-OH of glucose showed a hydrogen bond interaction with the side chain oxygen atom of Glu-256, the 2-NH group of the inhibitor does not form a hydrogen bond interaction due to small movements in the relative positions of Glu-256 and the inhibitor. The acetyl group also was not predicted to form any hydrogen bond interactions, although it contains a carbonyl group that is a potential hydrogen bond acceptor. Instead, the acetyl group of *N*-acetylglucosamine was predicted to form van der Waals interactions with the hydrophobic side chains of Pro-153 and Thr-168. The interaction energy of *N*-acetylglucosamine bound to the open conformation of glucokinase was calculated to be −67.8 kcal/mol or 8.2 kcal/mol more than the calculated interaction energy of glucose and glucokinase (Table 4).

The binding of mannoheptulose to glucokinase was predicted to resemble that of mannose, as shown in Figures 8b and 6b. Similar interactions were formed by the 1-OH, 2-OH, 3-OH, 4-OH, and 6-OH groups of both mannose and mannoheptulose. In addition, the 7-OH of mannoheptulose was predicted to form a hydrogen bond interaction with the side chain oxygen of Glu-290. This extra hydrogen bond

and other interactions of the 7-C and 7-OH resulted in the lower calculated interaction energy of −81.9 kcal/mol for mannoheptulose compared to the value of −75.5 kcal/mol for mannose with glucokinase (Table 4). Therefore, in the absence of solvation or entropic contributions, mannoheptulose would be predicted to bind more tightly than mannose to the open conformation of glucokinase.

DISCUSSION

The most distinctive feature of mammalian glucokinase is its high K_m for glucose and lack of physiologically relevant inhibition by the product, glucose 6-phosphate. The sugar specificity of human β-cell glucokinase had not been investigated nor are the determinants of this specificity understood for any mammalian hexokinase, although hexose specificity of the rat liver enzyme has been investigated (Neet et al., 1990; Cardenas et al., 1984a,b) and was similar to the human β-cell enzyme. Sugar specificity of the human β-cell hexose signaling enzyme, glucokinase, was investigated in order to begin to elucidate the basis for the enzyme's low affinity for glucose and its preference for various sugars. The four hexose sugars are all phosphorylated by glucokinase in the relative k_{cat}/K_m order of glucose = mannose > 2-deoxyglucose > fructose. These sugars, except for fructose,[2] induce an increase in the intrinsic fluorescence, which suggests that they exert similar conformational changes on the enzyme structure. Molecular modeling has been used to predict how each of these sugars binds to glucokinase using accurate molecular mechanics and dynamics minimization of a model based on the crystal structure of yeast hexokinase B. This new model included water molecules from the hexokinase crystal structure because several formed important interactions in the sugar binding site, as shown in Figure 6. This suggested that the positions of critical water molecules are conserved in both yeast hexokinase and glucokinase, and minimization without water molecules resulted in larger displacements of glucose binding residues compared to their positions in the yeast hexokinase crystal structure. This is not surprising since water molecules were also found to be important components of the sugar-binding sites of other proteins (Quiocho et al., 1989). Yeast hexokinase and human glucokinase share 31% identical amino acid residues, which suggests that the two enzyme structures will have common backbone structures with root mean square differences of about 1.5 Å (Chothia & Lesk, 1986). However, the functionally conserved glucose binding sites are composed almost entirely of identical residues. All potential hydrogen bond interactions with glucose involve identical residues in both enzymes. This suggested that the sugar-binding site of glucokinase can be modeled with high accuracy, as was determined by comparison of a model of HIV protease, based on the crystal of a protease related by 30% identical amino acid residues with the crystal structure of HIV protease (Weber, 1990). The excellent agreement between the calculated interaction energies and the ln (k_{cat}/K_m) values, with a correlation coefficient of 0.99, suggested that the models were correct for binding of these four sugar substrates to the open conformation of glucokinase. The molecular mechanics interaction energy does not include contributions due to solvation, conformation change, or entropy. However, the calculations were performed using accurate all-atom potentials, water molecules from the yeast hexokinase crystal structure, and all nonbonded terms without the usual cutoff. The high correlation between predictions and measured k_{cat}/K_m for the sugars, glucose, mannose, 2-deoxyglucose, and fructose suggested that not surprisingly these sugars, which are mostly stereoisomers, have similar solvation energies and entropy changes and that the enthalpic changes are more important contributions to the difference in free energy. It also suggested that these sugars are recognized by binding to the open conformation of glucokinase, which provides a binding site configured for either glucose or mannose, sugars that differ in the position of the 2-OH group (Figure 6).

These models suggest that glucokinase can bind two classes of sugars, and the interactions depend on the conformation of the 2-hydroxyl. The glucose 2-OH interacts with the Glu-256 side chain oxygen, while the equivalent OH of mannose or fructose interacts with the carbonyl oxygen of residue 151 instead. Both mannose and glucose are phosphorylated at very similar rates despite the differences in interactions of the 2-OH groups of the two sugars. However, only glucose and 2-deoxyglucose and not mannose or the other sugars induce cooperative behavior with Hill coefficients of 1.7 and 1.5, respectively (Xu et al., 1994b). This result with the human β-cell enzyme is quite different from that reported for the rat liver enzyme (Cardenas et al., 1984a,b). That form of glucokinase exhibited cooperativity with both glucose and mannose, with a Hill coefficient of 1.7, while both fructose and deoxyglucose had Hill coefficients of 1.0. The reason for the discrepancy is not known, but the difference demonstrates that, although these enzymes are highly conserved in sequence, they do exhibit differences in their cooperative behavior with various sugars. Cardenas et al. (1984a) postulated that the differences in cooperativity of the various substrates of the rat liver enzyme were a consequence of differences in velocities of conformational transitions induced by the different sugar substrates. These authors postulated that glucokinase exists mainly in one conformational state in the absence of hexose. Binding of glucose or any sugar that exhibits cooperativity was predicted to induce a conformational change. Presumably, this is reflected in the hexose-induced changes in intrinsic fluorescence. The new conformation was postulated to have a higher affinity for sugar substrate and higher catalytic activity. It should be noted that our results suggest that binding of substrates to the open form of the human enzyme accounts for the observed kinetic parameters. It was also postulated that inhibitors such as *N*-acetylglucosamine induce or trap the enzyme in the second conformation, even though this form is postulated to be more active. The data reported here on the human enzyme are consistent with this proposal for mannoheptulose and *N*-acetylglucosamine inhibition of the rat enzyme since both inhibitors increased intrinsic fluorescence. This slow transition model provides a kinetic explanation for some of the cooperative behavior of the enzyme but does not provide a molecular basis for the phenomena. Xu et al. (1994a) recently demonstrated that mutation of any glucose binding residue abolishes the cooperative behavior of the enzyme, and they postulated that cooperativity arose as a result of interaction of these highly conserved glucose binding residues with other parts of the enzyme subunit. The finding in this report that glucose and deoxyglucose exhibit cooperativity but fructose or mannose do not suggests that the interactions of glucose with human glucokinase, especially those of the 2-OH with Glu-256, are

critical for cooperativity or else that the interactions of mannose or fructose with the carbonyl oxygen of residue 151 prevent cooperativity. Recently, consistent with this hypothesis, Ser-151 has been shown to be importantly involved in cooperative behavior of human glucokinase (Xu et al., 1994a). We propose that the interaction of glucose binding residues (including Ser-151) with other regions of the protein may be responsible for the conformational transition proposed by Cardenas et al. (1984b).

Glucosamine has been shown to inhibit glucokinase in rat islet homogenates and to impair insulin secretion in isolated rat islets (Balkan et al., 1994). These workers concluded that glucosamine, via a reduction of glucokinase activity, impairs insulin secretion in a manner comparable to that seen in NIDDM. However, if glucosamine is metabolished, the product(s) of this metabolism may also influence glucose signaling of insulin release. No kinetic measurements of glucokinase with glucosamine as a substrate had appeared in the literature. We demonstrate here that, in addition to the well-known effect of this amino-sugar as an inhibitor of glucokinase, it is also a substrate. Yeast hexokinase has also been reported to phosphorylate other amino-sugars (Viola et al., 1982). Glucosamine binding to human glucokinase was predicted to be very similar to that of glucose; however, the calculated interaction energy does not agree well with the measured k_{cat}/K_m value (Table 4). This could arise in several ways since the molecular mechanics calculations did not include energies of solvation or entropic terms and were made using only the open conformation. Glucosamine has a charged amine group and is expected to have a different solvation energy to that of the uncharged glucose, mannose, and fructose. Glucosamine was shown to differ from the other sugars in the direction of the change that it induced in the intrinsic fluorescence, and it was observed to show a substrate inhibition at high concentrations. Therefore, it is not clear exactly how the glucosamine is interacting with the enzyme, nor what conformation is induced by the binding of glucosamine to glucokinase. In addition, the use of glucosamine as an inhibitor of insulin secretion in islet systems should be tempered with the caveat that this amino-sugar can be phosphorylated by glucokinase.

Interestingly, the inhibitors (*N*-acetylglucosamine and mannoheptulose) both induced an increase in the intrinsic fluorescence of glucokinase to almost the same extend as did 2-deoxyglucose but to a lower value than with glucose or mannose. This suggested that binding of these inhibitors to glucokinase induces a similar conformation change to that induced by glucose. Both are competitive inhibitors, with measured K_i's of 0.20 mM for *N*-acetylglucosamine and 0.76 mM for mannoheptulose. The measured K_i values do not correlate well with the calculated interaction values of −67.8 and −81.9 kcal/mol for *N*-acetylglucosamine and mannoheptulose, respectively. This may be due to differences in the solution energies, and entropic changes, which were not calculated, or the inhibitory effect may be exerted in the closed conformation of glucokinase. Both inhibitors contain additional groups compared to the substrate sugars: the acetyl group of *N*-acetylglucosamine and the 7-CH_2OH of mannoheptulose. In the model structure, these extra groups are directed toward the open side of the cleft as is the *o*-tolulyl group of the hexokinase inhibitor (OTG) and may block completion of the conformation change and/or the next stage of the reaction.

Incubation of yeast hexokinase with [γ^{32}-P]ATP resulted in hydrolysis of the γ-phosphate and labeling of the enzyme on Ser-158 (Menezes & Pudles, 1976; Kuromizu et al., 1979). Human glucokinase also exhibited an ATPase activity concomitant with phosphate incorporation into the enzyme. The lack of effect of the pentose (lyxose) on glucokinase-associated ATPase activity may provide a clue for explaining the low affinity of the enzyme for various hexose sugars. The ATPase activity of yeast hexokinase is 1/10000th that of the glucose phosphorylation reaction rate while that for glucokinase is 1/2000th the V_{max} of the kinase reaction, although the K_m for ATP is the same for both enzymes (DelaFuente et al., 1970). The higher glucokinase ATPase rate suggests that water molecules are more accessible to the terminal phosphate of ATP in the absence of glucose than is the case for the yeast enzyme. In yeast hexokinase, when the nonphosphorylatable sugar lyxose occupies the sugar binding site, ATPase V_{max} is increased by a factor of 10. This change is presumably due to a conformational change induced in the enzyme by the substrate-like sugar. The higher ATPase activity of glucokinase and lack of effect of lyxose may reflect a difference in its active site conformation compared to that of the yeast enzyme, and higher concentrations of glucose are presumably necessary to induce the conformational change required for efficient phosphotransferase activity. Interestingly, Ser-151 corresponds to the yeast enzyme Ser-158, which is phosphorylated during ATP hydrolysis. Ser-151 may undergo phosphorylation and/or be involved in the cooperative behavior of the enzyme and its lower affinity for glucose (Xu et al., 1994a). Work is in progress to determine the basis for the much lower affinity for hexose of glucokinase relative to that for yeast and the low K_m mammalian hexokinases by employing a combination of fluorescence techniques and site-directed mutagenesis.

ACKNOWLEDGMENT

The authors wish to thank Michele Leva and Kristina Johnson for their skillful typing of the manuscript and Loren Runnels for assistance with the fluorescence experiments. The authors would like to thank Dr. W. W. Cleland (Enzyme Institute, University of Wisconsin) for constructive criticism during the preparation of this manuscript.

REFERENCES

Anderson, C. M., Zucker, F. H., & Steitz, T. A. (1979) *Science 204*, 375−380.

Andreone, T., Printz, R. L., Pilkis, S. J., Magnuson, M. A., & Granner, D. K. (1989) *J. Biol. Chem. 264*, 363−369.

Cardenas, M. L., Rabajille, E., & Niemeyer, H. (1984a) *Biochem. J. 222*, 363−370.

Cardenas, M. L., Rabajille, E., & Niemeyer, H. (1984b) *Eur. J. Biochem. 145*, 163−17.

Chan, C. B. (1993) *Biochemical J. 295*, 673−677.

Charles, R. S., Harrison, R. W., Bell, G. I., Pilkis, S. J., & Weber, I. T. (1994) *Diabetes 43*, 784−791.

Chothia, C., & Lesk, A. M. (1986) *EMBO J. 5*, 823−826.

Cleland, W. W. (1979) *Methods Enzymol. 63*, 500−513.

DelaFuente, G., Lagunas, R., & Sols, A. (1970) *Eur. J. Biochem. 16*, 226−233.

Ferrer, J., Gomis, R., Fernandez Alvarez, J., Casamitjana, R., & Vilardell, E. (1993) *Diabetes 42* (9), 1273−1280.

Gidh-Jain, M., Takeda, J., Xu, L. Z., Lange, A. J., Vionnet, N., Stoffel, M., Froguel, P., Velho, G., Sun, F., Cohen, D., Patel, P., Lo, Y.-M. D., Hattersley, A. T., Luthman, H., Wedell, A.,

St. Charles, R., Harrison, R. W., Weber, I. T., Bell, G. I., & Pilkis, S. J. (1993) *Proc. Natl. Acad. Sci. U.S.A. 90*, 1932−1956.
Granner, D. K., & Pilkis, S. J. (1990) *J. Biol. Chem. 265*, 16012−16016.
Harrison, R. W. (1985) Refinement of Yeast Hexokinase A and B Crystal Structure. Ph.D. Thesis, Yale University, New Haven, CT.
Harrison, R. W. (1993) *J. Comput. Chem. 14*, 1112−1122.
Jones, A. T. (1985) *Methods Enzymol. 115*, 157−171.
Kuromizu, K., Cheng, L.-Y., Takahashi, N., Fletcher, P., Inagami, T., & Colowick, S. P. (1979) *Fed. Proc. 35*, 302.
Lange, A. J., Xu, L. Z., Van Poelwijk, F., Granner, D. K., & Pilkis, S. J. (1991) *Biochem. J. 277*, 159−163.
Lin, K., Kurland, I. J., Xu, Z., Lange, A. J., Pilkis, J., El-Maghrabi, M. R., & Pilkis, S. J. (1990) *Protein Expression Purif. 1*, 169−176.
Lin, S. X., & Neet, E. K. (1990) *J. Biol. Chem. 265*, 9670−9675.
Meglasson, M. D., & Matchinsky, F. M. (1986) *Diabetes/Metab. Rev. 2*, 163−214.
Menezes, L. C., & Pudles, J. (1976) *Eur. J. Biochem. 65*, 41−47.
Neet, K. E., Keenan, R. P., & Tippett, P. S. (1990) *Biochemistry 29*, 770−777.
Polonsky, K. S., Licinio-Paixao, J., Given, B. D., Pugh, W., Rue, P., Galloway, J., Karnson, T., & Frank, B. (1986) *J. Clin. Invest. 77*, 98−105.
Quiocho, F. A., Wilson, D. K., & Vyas, N. K. (1989) *Nature 340*, 404−407.
Rappe, A. K., & Goodard, W. A., III. (1991) *J. Chem. Phys. 95*, 3358−3363.
Rappe, A. K., Casewit, C. J., Colwell, K. S., Goddard, W. A., III, & Skiff, W. M. (1992) *J. Am. Chem. Soc. 114*, 10024−10035.
Stoffel, M., Froguel, P., Takeda, J., Zouali, H., Vionnet, N., Nishi, S., Weber, I., T., Harrison, R. W., Pilkis, S. J., Lesage, S., Vaxillaire, M., Velho, G., Sun, F., Iris, F., Passa, P., Cohen, D., & Bell, G. I. (1992a) *Proc. Natl. Acad. Sci. U.S.A. 89*, 7698−7702.
Stoffel, M., Patel, P., Lo, Y.-M.D., Hattersley, A. T., Lucassen, A. M., Page, R., Bell, J. I., Bell, G. I., Turner, R. C., & Wainscoat, J. S. (1992b) *Nat. Genet. 2*, 153−156.
Studier, F. W., & Moffat, B. A. (1986) *J. Mol. Biol. 189*, 113−130.
Sturis, J., Kurland, I. J., Byrne, M. M., Mosekilde, E., Froguel, P., Pilkis, S. J., Bell, G. I., & Polonsky, K. S. (1994) *Diabetes 43*, 718−723.
Takeda, J., Gidh-Jain, M., Xu, L. Z., Froguel, P., Velho, G., Vaxillaire, M., Cohen, D., Shimada, F., Makino, H., Nishi, S., Stoffel, M., Vionnet, N., St. Charles, R., Harrison, R. W., Weber, I. T., Bell, G. I., & Pilkis, S. J. (1993) *J. Biol. Chem. 268*, 15200−15204.
Viola, R. E., Raushel, F. M., Rendina, A. R., & Cleland, W. W. (1982) *Biochemistry 21*, 1295−1302.
Vionnet, N., Stoffel, M., Takeda, J., Yasuda, K., Bell, G. I., Zouali, H., Lesage, S., Velho, G., Iris, F., Passa, P., Froguel, P., & Cohen, D. (1992) *Nature 356*, 721−722.
Weber, I. T. (1990) *Proteins: Struct. Funct. Genet. 7*, 172−184.
Weiner, S. J., Kollman, P. A., Nguyen, D. T., & Case, D. A. (1986) *J. Comput. Chem. 7*, 230−252.
Weinhouse, S. (1976) *Curr. Top. Cell Regul. 11*, 1−69.
Xu, L. Z., Weber, I. T., Harrison, R., & Pilkis, S. J. (1994a) *J. Biol. Chem.* (in press).
Xu, L. Z., Zhang, W., Weber, I. T., Harrison, R., & Pilkis, S. J. (1994b) *J. Biol. Chem. 269*, 27458−27465.

BI9424611